

# Design of star-shaped molecular architectures based on carbazole and phosphine oxide moieties: towards amorphous bipolar hosts with high triplet energy for efficient blue electrophosphorescent devices

Junqiao Ding,<sup>a</sup> Qi Wang,<sup>ab</sup> Lei Zhao,<sup>a</sup> Dongge Ma,<sup>a</sup> Lixiang Wang,<sup>\*a</sup> Xiabin Jing<sup>a</sup> and Fosong Wang<sup>a</sup>

Received 27th March 2010, Accepted 29th June 2010

DOI: 10.1039/c0jm00846j

With a carbazole moiety as the electron donor and a phosphine-oxide moiety as the electron acceptor, two novel star-shaped bipolar hosts, 4,4',4''-tri(*N*-carbazolyl)triphenylphosphine oxide (TCTP) and 3,6-bis(diphenylphosphoryl)-9-(4'-(diphenylphosphoryl)phenyl)carbazole (TPCz), have been designed and synthesized. Their topology structure differences are that the phosphine-oxide moiety is located in the molecular centre and the periphery for TCTP and TPCz, respectively. The star-shaped architecture imparts them with high decomposition temperatures ( $T_d$ : 497 °C for TCTP and 506 °C for TPCz) and results in the formation of a stable amorphous glassy state ( $T_g$ : 163 °C for TCTP and 143 °C for TPCz), while the phosphine oxide linkage ensures the disrupted conjugation and the high triplet energy (>3.0 eV). In addition, both TCTP and TPCz possess a bipolar transporting capability. However, TCTP mostly transports holes and TPCz primarily conducts electrons. On the basis of appropriate device configurations, high performance blue electrophosphorescent devices with comparable efficiency (35.0–36.4 cd A<sup>-1</sup>, 15.9–16.7%) have been realized using TCTP and TPCz as the host for the blue phosphor, respectively. Compared with the unipolar host, 4,4',4''-tri(*N*-carbazolyl)triphenylamine (TCTA, 15.9 cd A<sup>-1</sup>, 7.8%), the efficiency is improved by more than two-fold. As far as the obtained state-of-the-art performance is concerned, we think that these novel materials should provide an avenue for the design of amorphous bipolar hosts with high triplet energy used for blue PhOLEDs on a star-shaped scaffold.

## 1. Introduction

For a potential application in solid state lighting,<sup>1</sup> phosphorescent organic light-emitting diodes (PhOLEDs) have attracted much attention due to their possibility to achieve comparable or even higher power efficiencies than fluorescent tubes.<sup>2</sup> However, as one of the components necessary for white light, the performance of the blue PhOLEDs is not as good as the corresponding red and green ones,<sup>3–9</sup> where the host material remains a challenge. To be an effective host of the blue phosphor suitable for vacuum deposition technology, three key factors must be considered together. Firstly, the host should possess an amorphous film morphology to ensure the device reproducibility and stability.<sup>10</sup> Hence, a nonplanar star-shaped structure, which has been previously demonstrated to be a successful strategy to obtain organic glasses,<sup>11</sup> could be employed in the design of the amorphous host. Secondly, the triplet energy of the host is required to be higher than 2.75 eV<sup>12</sup> in order to prevent the back energy transfer from the phosphor to the host.<sup>13</sup> Finally, a significant point to emphasize is the capability of the host to transport both holes and electrons, which is of paramount importance to maintain the charge balance in the emissive layer (EML) so as to improve the device efficiency accompanied by a small roll-off.<sup>14,15</sup> A desirable, bipolar host containing suitable

electron-rich and -deficient moieties in one molecule has been intensely studied by several groups.<sup>16–18</sup> Considering all these features, therefore, we aim to develop the novel amorphous bipolar hosts with high triplet energy used for the blue PhOLEDs.

To date, a star-shaped molecule, 4,4',4''-tri(*N*-carbazolyl)triphenylamine (TCTA), has been widely used as the host of the phosphors.<sup>2,5,19,20</sup> Nevertheless, it only behaves as a unipolar hole-transporter. On the other hand, some reported molecules containing phosphine oxide have been demonstrated to predominantly transport electrons.<sup>21–23</sup> From the molecular design aspect, it is reasonable to replace the nitrogen atom in TCTA with phosphine oxide to afford a bipolar host,

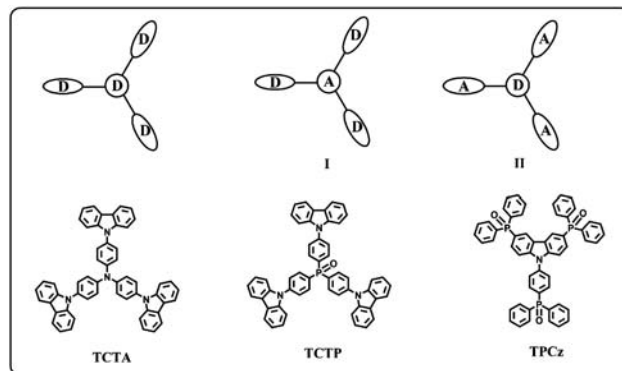


Fig. 1 Schematic representations of the hosts and their corresponding molecular structures.

<sup>a</sup>State Key Laboratory of Polymer Physics and Chemistry, Changchun Institute of Applied Chemistry, Chinese Academy of Sciences, Changchun, 130022, P. R. China. E-mail: lixiang@ciac.jl.cn; Fax: (+86)0431-8568-5653

<sup>b</sup>Graduate School of the Chinese Academy of Sciences, Beijing, 100039, P. R. China

4,4',4''-tri(*N*-carbazolyl)triphenylphosphine oxide (TCTP). As shown in Fig. 1, TCTP is associated with topology structure I, in which the electron acceptor (A), the phosphine oxide moiety, is used as the core and the electron donor (D), the carbazole moiety, acts as the branch. In view of the star-shaped scaffold, there exists another inverted architecture, topology structure II, where A locates at the molecular periphery and D locates in the molecular center. Consequently, 3,6-bis(diphenylphosphoryl)-9-(4'-(diphenylphosphoryl)phenyl)carbazole (TPCz), with a phosphine oxide moiety as the branch and a carbazole moiety as the core, is simultaneously designed. It is worth noting that, for both TCTP and TPCz, the disrupted conjugation *via* phosphine-oxide linkage can be well-preserved to ensure their high triplet energies.

Although the bipolar hosts containing phosphine oxide have been reported recently,<sup>23,24</sup> few endeavors have been paid to the development of the amorphous star-shaped bipolar hosts, which are believed to show better thermal and morphology stability. In this article, based on carbazole and phosphine-oxide moieties, TCTP and TPCz were conveniently synthesized, and the effect of the topology structure on their thermal, photophysical, electrochemical, bipolar transporting and device properties was investigated in detail.

## 2. Results and discussion

### 2.1 Synthesis and chemical characterization

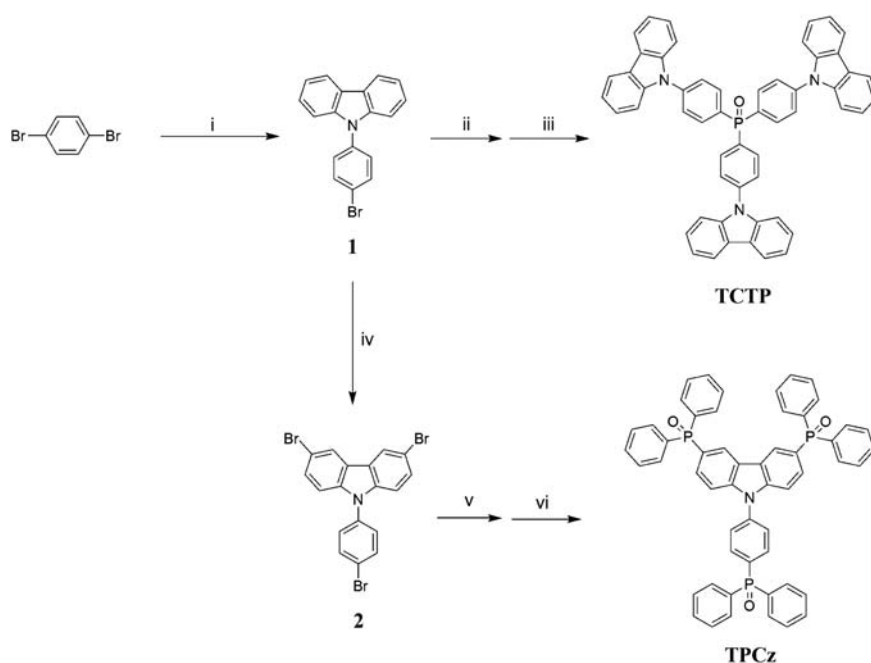
Scheme 1 outlines the synthesis of the bipolar hosts, TCTP and TPCz. The key intermediate 9-(4'-bromophenyl)carbazole (**1**) was synthesized by a modified Ullmann reaction.<sup>6</sup> Further bromination with *N*-bromosuccinimide (NBS) gave another important intermediate 9-(4'-bromophenyl)-3,6-dibromocarbazole (**2**). Then, TCTP was prepared from **1** with a total yield of

41% sequentially through a lithium-halogen exchange reaction with *n*-butyllithium, a coupling reaction with trichlorophosphine and an oxidation reaction with hydrogen peroxide. Similarly, TPCz was obtained from **2** and chlorodiphenylphosphine with a yield of 47%. Both TCTP and TPCz were purified by column chromatography and their structures were confirmed with <sup>1</sup>H NMR, <sup>13</sup>C NMR, <sup>31</sup>P NMR, elemental analysis and MALDI-TOF mass spectroscopy. Before device fabrication, both TCTP and TPCz were further purified by sublimation. For comparison, TCTA was also synthesized as the model compound.

From the <sup>31</sup>P NMR spectrum of TCTP, only one signal peak ( $\delta = 27.5$  ppm) was observed. However, the <sup>31</sup>P NMR spectrum of TPCz revealed two distinct signals,  $\delta = 28.4$  and 30.1 ppm. According to the signal intensity, the former peak could be ascribed to the 4'-positioned P atom of the *N*-phenyl ring, and the latter was related to the 3 and 6-position P atoms of the carbazole unit. The upfield shift shows the higher electron density of the 4'-positioned P atom compared with the 3 and 6-positions.

### 2.2 Thermal and photophysical properties

The thermal properties of TCTP and TPCz with respect to TCTA were estimated by differential scanning calorimetry (DSC) and thermogravimetric analysis (TGA). Fig. 2 displays their DSC curves recorded over the temperature range 50–350 °C. For all the sublimated samples during the first heating process, only an endothermic peak due to melting appeared. On the second heating, the DSC of TCTA revealed a glass transition ( $T_g = 152$  °C), followed by an exotherm at 237 °C caused by crystallization and an endotherm at 268 °C associated with melting. As for TCTP and TPCz, however, an amorphous glassy state was formed upon cooling from the melt. After heating



**Scheme 1** Synthesis of the bipolar hosts. Reagents and conditions: (i) carbazole, CuI, K<sub>2</sub>CO<sub>3</sub>, 1,3-dimethyl-3,4,5,6-tetrahydro-2(1H)-pyrimidinone (DMPU), 18-crown-6, 190 °C; (ii) *n*-BuLi, THF, PCl<sub>3</sub>, –78 °C; (iii) 30% H<sub>2</sub>O<sub>2</sub>, CH<sub>2</sub>Cl<sub>2</sub>; (iv) *N*-bromosuccinimide (NBS), dimethylformamide (DMF), 0 °C; (v) *n*-BuLi, THF, chlorodiphenylphosphine, –78 °C; (vi) 30% H<sub>2</sub>O<sub>2</sub>, CH<sub>2</sub>Cl<sub>2</sub>.

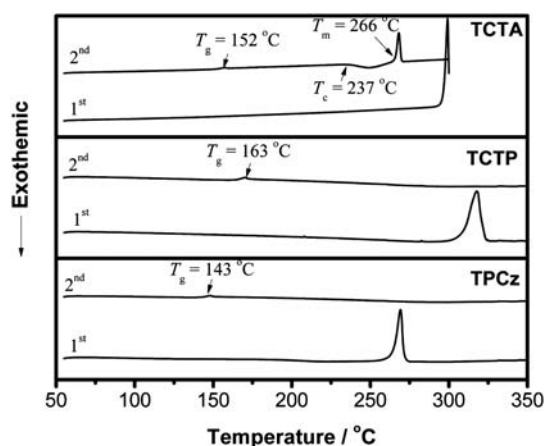


**Fig. 2** DSC curves of the hosts (heating rate: 20 °C min<sup>-1</sup>).  $T_g$ : glass-transition temperature;  $T_c$ : crystallization temperature;  $T_m$ : melting-point temperature.

again, a well-defined glass transition occurred at 163 and 143 °C for TCTP and TPCz, respectively, and no exothermic peak related to crystallization was observed at temperatures up to 350 °C. These observations indicate that the enhanced thermal stability of the amorphous glass states of TCTP and TPCz may arise from the repulsive effect of the additional oxygen atom, which causes the more crowded arrangement of the aryl groups around the P atom, and prevents the easy intermolecular packing and hence ready crystallization. In addition, TCTP and TPCz exhibited a decomposition temperature of 497 and 506 °C, respectively, about 8–17 °C higher than that of TCTA ( $T_d = 489$  °C).

Upon going from TCTA to TCTP, this repulsive effect from the oxygen atom can also lead to the decrease of the molecular conjugation length after the replacement of the N atom in TCTA with phosphine oxide. For example, an obvious blue shift for the lowest-energy absorption bands in the range 300–360 nm is clearly seen in Fig. 3, and thus the optical band gap ( $E_g$ ) estimated from the onset of the absorption spectra increases from 3.46 eV of TCTA to 3.58 eV of TCTP (Table 1). Correspondingly, the

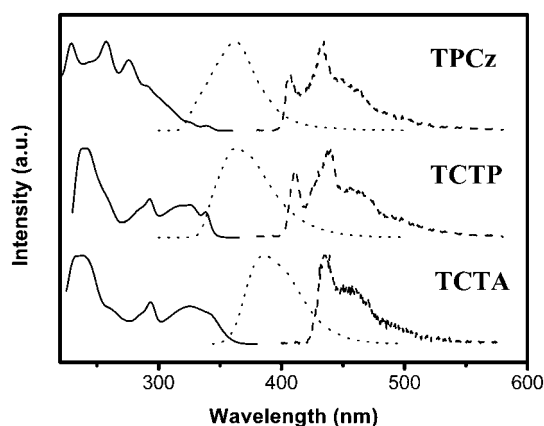


**Fig. 3** The absorption spectra (—) in dichloromethane solutions and PL spectra (···) in toluene solutions at 298 K, and the phosphorescence spectra (---) at 77 K of the hosts.

emission maximum of TCTP is blue-shifted by about 23 nm. Moreover, the triplet energy estimated from the highest energy peak of the phosphorescence spectra at 77 K enhances by about 0.18 eV from TCTA to TCTP. As a result, TCTP gives a triplet energy as high as 3.03 eV, which is sufficient to host the blue phosphor, iridium(III)[bis(4,6-difluorophenyl)-pyridinato-*N,C*]-picolinate (FIrpic, 2.65 eV). This enhanced triplet energy, which suggests potentially effective prevention of the back energy transfer from the phosphor to the host,<sup>13</sup> is a very desirable feature for PhOLEDs. In contrast, the shifts of the absorption and emission spectra are almost negligible when going from TCTP to TPCz. This demonstrates that the photophysical properties are hardly influenced by their topology structure, no matter if the phosphine oxide moiety locates in the center or at the periphery of the architecture.

### 2.3 Electrochemical properties, theoretical calculations and bipolar transporting characteristics

The cyclic voltammograms (CV) were measured in dichloromethane to study the energy levels of the hosts. The highest occupied and lowest unoccupied molecular orbital (HOMO/LUMO) energy levels can be calculated from the electrochemical data together with the absorption spectra, and the data are summarized in Table 1. Interestingly, TCTP and TPCz display different redox behavior. During the anodic and cathodic scans, there are two quasi-reversible oxidation waves and no reduction waves for TCTP in Fig. 4. As for TPCz, however, only irreversible reduction waves are detected. In comparison to TPCz, TCTP has a much higher HOMO energy level of  $-5.25$  eV, indicative of its effective hole injection capability. In contrast, a much lower LUMO energy level of  $-2.69$  eV for TPCz is obtained, which suggests that electrons are more easily injected from the cathode.

To further understand the effect of the topology structure on the electronic properties, density functional theory (DFT) calculations were carried out using B3LYP hybrid functional theory with 6-31G\* basis sets (see Experimental). The optimized structures and the HOMO/LUMO distribution for TCTP and TPCz are given in Fig. 5. As can be seen from Fig. 5, the HOMO and LUMO of TCTP are separately distributed over the periphery carbazole units and the central triphenyl phosphine oxide, respectively. However, the situation is entirely opposite for TPCz, for its HOMO mainly consists of the highest  $\pi$ -orbitals of the carbazole moiety located in the center, while its LUMO mostly corresponds to the lowest  $\pi$ -orbitals of the periphery triphenyl phosphine oxide at the *N*-position of the carbazole moiety. This result is consistent with the higher electron density of the 4'-positioned P atom observed in the <sup>31</sup>P NMR spectrum of TPCz.

Combining their electrochemical behavior with the HOMO and LUMO distribution, we can postulate that TCTP is favorable for the hole injection and transporting, while TPCz is suitable for the electron injection and transporting. To verify our hypothesis, the same device structure (Fig. 6) with a 10 nm thick film of TCTA, TCTP, or TPCz inserted between *N,N'*-bis(1-naphthyl)-*N,N'*-diphenyl-1,1'-biphenyl-4,4'-diamine (NPB) and tris(8-hydroquinolinato)aluminium (Alq<sub>3</sub>) was adopted according to the literature.<sup>25</sup> Fig. 6 shows their electroluminescence

**Table 1** The thermal, photophysical and electrochemical properties of the hosts

	$T_g/T_d/T_m$ <sup>a</sup> /°C	$T_d$ <sup>b</sup> /°C	$\lambda_{\text{abs}}$ (log $\epsilon$ ) <sup>c</sup> /nm	$\lambda_{\text{em}}$ <sup>d</sup> /nm	$T_1$ <sup>e</sup> /eV	$E_g$ <sup>f</sup> /eV	HOMO/eV	LUMO/eV
TCTA	152; 237; 266	489	238 (5.1), 293 (4.8), 326 (4.6)	386	2.85	3.46	-5.09	-1.63
TCTP	163; —; —	497	233 (5.2), 292 (4.7), 326 (4.6), 338 (4.5)	363	3.03	3.58	-5.25	-1.67
TPCz	143; —; —	506	229 (4.8), 258 (4.8), 276 (4.6)	363	3.07	3.58	-6.27	-2.69

<sup>a</sup> Data obtained from the second DSC scans. <sup>b</sup> The temperature at which 5% weight loss was detected. <sup>c</sup> Measured in CH<sub>2</sub>Cl<sub>2</sub> at 298 K with a concentration of 10<sup>-5</sup> M. <sup>d</sup> Measured in toluene at 298 K with a concentration of 10<sup>-5</sup> M and an excitation wavelength of 330 nm. <sup>e</sup> Estimated from the highest energy peak of the phosphorescence spectra at 77 K. <sup>f</sup> Estimated from the onset of the absorption spectrum. HOMO = -e (4.8 V +  $E^{\text{ox}}$ ), LUMO = -e (4.8 V +  $E^{\text{red}}$ ), and LUMO =  $E_g$  + HOMO, where  $E^{\text{ox}}$  and  $E^{\text{red}}$  were taken from the onset of the oxidation and reduction potential, respectively.

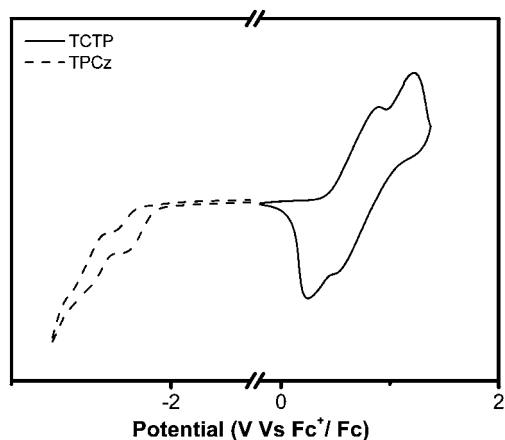


**Fig. 4** The cyclic voltammograms of TCTP and TPCz. Scan rate = 50 mV s<sup>-1</sup>; solvent = dichloromethane; concentration = 1 mM.

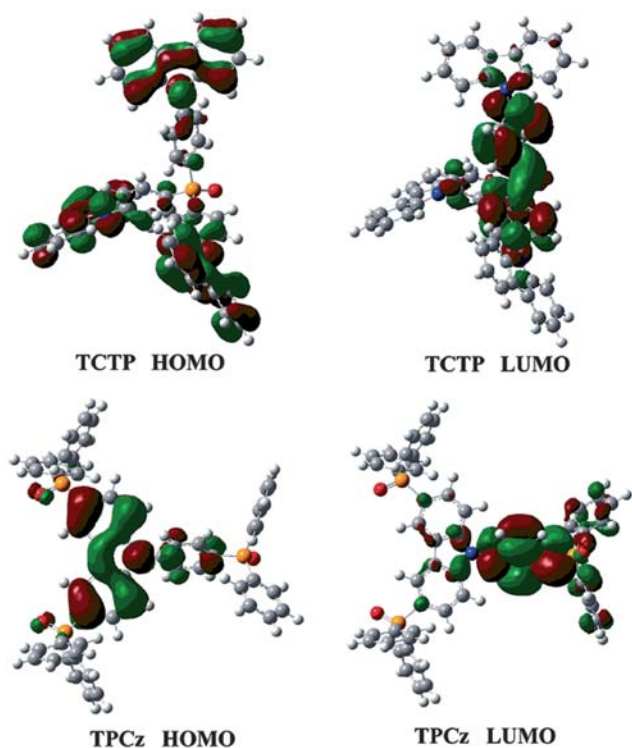


**Fig. 5** Molecular simulation results of TCTP and TPCz, showing the HOMO and LUMO distribution.

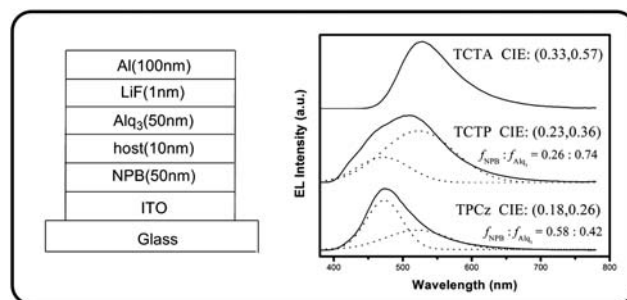


**Fig. 6** Electroluminescent spectra of devices with a configuration of ITO/NPB(50nm)/TCTA, TCTP, or TPCz (10nm)/Alq<sub>3</sub>(50nm)/LiF(1nm)/Al(100nm) measured at a driving voltage of 10 V. The dotted lines are the fitted emissions corresponding to NPB and Alq<sub>3</sub>.

(EL) spectra at a driving voltage of 10 V. It can be clearly seen that the EL spectrum of the TCTA-based device was completely dominated by the emission of Alq<sub>3</sub> with the Commission Internationale de L'Eclairage (CIE) coordinates of (0.33, 0.57). However, for the TCTP-based device, the emissions from both Alq<sub>3</sub> and NPB with a ratio of 0.74 : 0.26 were observed, and the corresponding CIE coordinates blue-shifted to (0.23, 0.36). Furthermore, for TPCz-based device, the ratio of the emission coming from NPB further increased from 26% to 58% accompanied by the CIE coordinates shifting to (0.18, 0.26). These observations indicate that the TCTA interlayer only transports holes, whereas the TCTP and TPCz layers permit both electrons and holes to pass. That is to say, both TCTP and TPCz exhibit a bipolar transporting nature. Nevertheless, as discussed above, TCTP mostly transports holes, and TPCz primarily transports electrons.

## 2.4 Electrophosphorescent OLED characterization

### 2.4.1 TCTP-based blue electrophosphorescent devices.

The bipolar transporting characteristic as well as the excellent morphology stability and high triplet energy suggests that TCTP and TPCz can be used as the ideal hosts for the blue electrophosphorescent devices. Therefore, their electroluminescent properties were investigated using FIrpic as the corresponding blue dopant.

As indicated in Fig. 7, device I was fabricated using TCTP as the host with a configuration of ITO/NPB (70 nm)/TCTA (5 nm)/8 wt% FIrpic: TCTP (20 nm)/TAZ (40 nm)/LiF (1 nm)/Al (100 nm). Here, NPB and TCTA were used as the hole

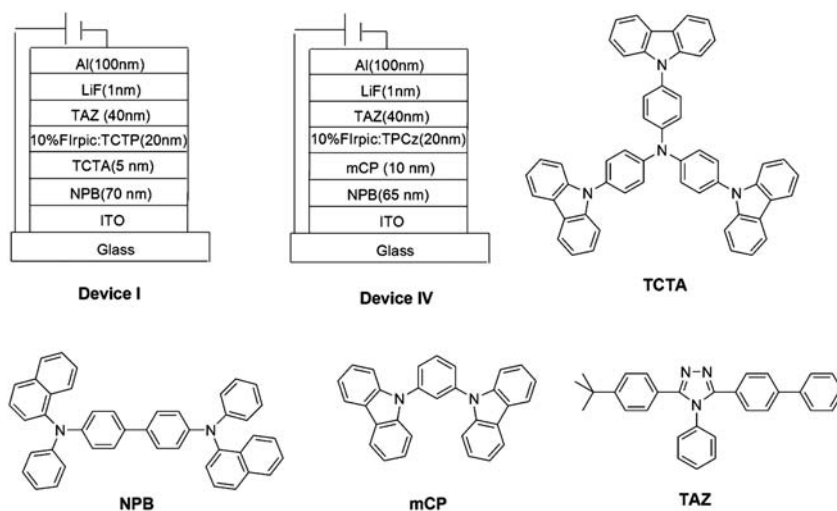


Fig. 7 A schematic diagram of EL device configurations and the molecular structures of the relevant compounds used in these devices.

transporting materials, and 3-(4-biphenyl)-4-phenyl-5-(4-*tert*-butylphenyl)-1,2,4-triazole (TAZ) was used as the electron transporting material. For comparison, the control device II: ITO/NPB (70 nm)/TCTA (5 nm)/8 wt% FIrpic: TCTA (20 nm)/TAZ (40 nm)/LiF (1 nm)/Al (100 nm) was also prepared.

Fig. 8 depicts the current density-voltage-luminance characteristics of devices I–II, and the EL spectrum of device I. The EL spectrum of device I shows the CIE coordinates of (0.15, 0.34), corresponding to the emission of FIrpic. Moreover, no additional emission from TCTP is observed, which demonstrates that the exciton energy can be efficiently transferred from TCTP to FIrpic. As presented in Fig. 8, device I and II have a similar turn-on voltage (voltage at  $1 \text{ cd m}^{-2}$ ) of about 3.2 V, but the current and the luminance of device I are higher than those of device II at the same driving voltage. For instance, the maximum luminance of device I and II are 35 100 and 5500  $\text{cd m}^{-2}$ , respectively. At the same time, the peak luminous efficiency increases from 15.9  $\text{cd A}^{-1}$  of TCTA to 35.0  $\text{cd A}^{-1}$  of TCTP, and a more than two-fold improvement is achieved (Fig. 9a). Correspondingly, the external quantum

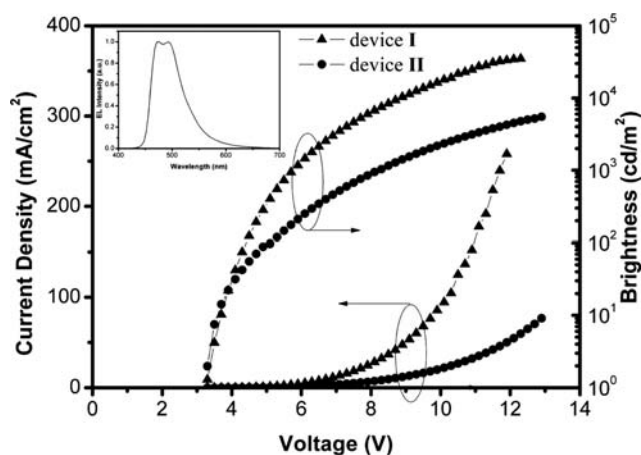


Fig. 8 Comparison of the current density-voltage-luminance characteristics between device I and II. Inset: the EL spectrum at a voltage of 8 V of device I.

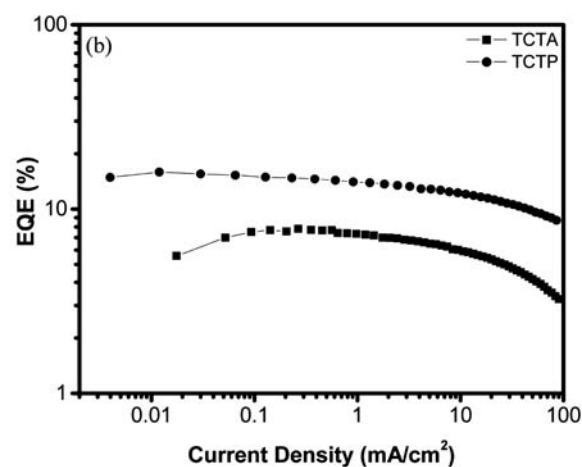
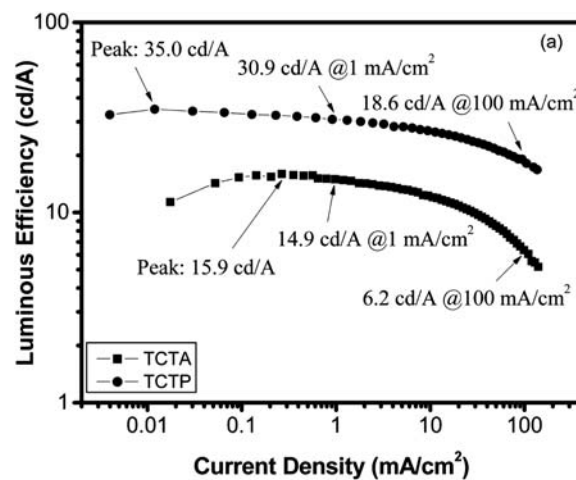


Fig. 9 Comparison of the current density dependence of the luminous efficiency (a) and EQE (b) between device I and II. In (a), the arrows indicate the maximum luminous efficiency, as well as the efficiency at 1 and 100  $\text{mA cm}^{-2}$ , respectively.

efficiency (EQE) of TCTP (15.9%) is about double that of TCTA (7.8%) (Fig. 9b). Furthermore, it is found that at high current density, the efficiency of TCTP decays more slowly than that of TCTA. For example, on going from 1 to 100 mA cm<sup>-2</sup>, the efficiency decreases by about 58 and 40% for TCTA and TCTP, respectively. The obtained small roll-off can be mainly attributed to the bipolar nature of TCTP. Owing to the conductivity of holes and electrons simultaneously through the whole EML, the excitons are believed to be formed in the bulk EML rather than located at the narrow interface. Consequently, the density of the triplet excitons can be controlled at a relatively low level to minimize the triplet-triplet (T-T) annihilation, and thus prohibit the steep efficiency roll-off.<sup>26,27</sup>

**2.4.2 TPCz-based blue electrophosphorescent devices.** To investigate the host capability of TPCz, device **III** was fabricated with an OLED structure: ITO/NPB (65 nm)/8 wt% FIrpic: TPCz (20 nm)/TAZ (40 nm)/LiF (1 nm)/Al (100 nm). Unfortunately, a very low efficiency of 0.75 cd A<sup>-1</sup> (0.3%) was obtained (Fig. 10). Taking into account the fact that TPCz can conduct electrons well, this is understandable. The injected electrons from the cathode can easily pass through the EML and enter into NPB layer, this inevitably results in the loss of the excited excitons and thus low efficiency. In order to suppress such undesirable loss, an

additional thin hole-transporting and electron-blocking layer should be inserted between the NPB and EML. Because of its high LUMO energy level (-1.5 eV),<sup>28</sup> *N,N'*-dicarbazolyl-3,5-benzene (mCP) was selected to block electrons, and device **IV** (ITO/NPB (65 nm)/mCP (10 nm)/8 wt% FIrpic: TPCz (20 nm)/TAZ (40 nm)/LiF (1 nm)/Al (100 nm)) was prepared (Fig. 7). As expected, device **IV** gave an efficiency of 36.4 cd A<sup>-1</sup> (16.7%), which is comparable with that of device **I**. This suggests that, although TCTP and TPCz have different bipolar transporting ability, they both can be used as an effective host for the fabrication of high-performance blue PhOLEDs with appropriate device configurations. In addition, compared with device **III**, the efficiency of device **IV** is enhanced by about 47 times, indicating the above-mentioned excellent electron-transporting ability of TPCz. Therefore, we used TPCz as the electron transporting material instead of TAZ to fabricate device **V**: ITO/NPB (65 nm)/mCP (10 nm)/8 wt% FIrpic: TPCz (20 nm)/TPCz (40 nm)/LiF (1 nm)/Al (100 nm). As shown in Fig. 10, the efficiency of device **V** still remains as high as 27.6 cd A<sup>-1</sup> (12.7%), close to that of device **IV**. This promising result has prompted us to further study the potential application of TPCz as the electron transporting material, and the detailed work will be reported elsewhere.

### 3. Conclusion

In summary, with a carbazole moiety as the electron donor and a phosphine oxide as the electron acceptor, we have demonstrated the design and synthesis of two novel star-shaped bipolar hosts, TCTP and TPCz. In terms of their amorphous morphology, high triplet energy and bipolar transporting characteristic, high performance blue electrophosphorescent devices with comparable efficiency have been realized using TCTP and TPCz as the hosts of the blue phosphor. Most importantly, these novel materials should provide an avenue for the design of the amorphous bipolar hosts with high triplet energy used for blue PhOLEDs based on the star-shaped scaffold.

### 4. Experimental

#### Synthesis

All chemicals and reagents were used as received from commercial sources without further purification. Solvents for chemical synthesis were purified according to the standard procedures. All chemical reactions were carried out under an inert atmosphere. 4,4',4''-tri(*N*-carbazolyl)triphenylamine (TCTA) was prepared according to the literature procedures.<sup>29</sup>

**Synthesis of 9-(4'-bromophenyl)carbazole (1).** A mixture of 1,4-dibromobenzene (14.2 g, 60.0 mmol), carbazole (5.0 g, 30.0 mmol), CuI (0.3 g, 1.5 mmol), 18-crown-6 (0.4 g, 1.5 mmol), K<sub>2</sub>CO<sub>3</sub> (6.24 g, 45.0 mmol) and 1,3-dimethyl-3,4,5,6-tetrahydro-2(1H)-pyrimidinone (DMPU) (6 mL) was heated at 190 °C for 24 h under argon. After cooling to room temperature, the reaction was quenched with 1 N hydrochloric acid. The mixture was extracted with CH<sub>2</sub>Cl<sub>2</sub>, washed with NH<sub>3</sub>·H<sub>2</sub>O and water, and dried over Na<sub>2</sub>SO<sub>4</sub>. After the solvent had been completely removed, the residue was purified by column chromatography on silica gel using petroleum as eluent to give 9-(4'-bromophenyl)carbazole (**1**) with a yield of 59% (5.7 g). <sup>1</sup>H NMR (CDCl<sub>3</sub>):

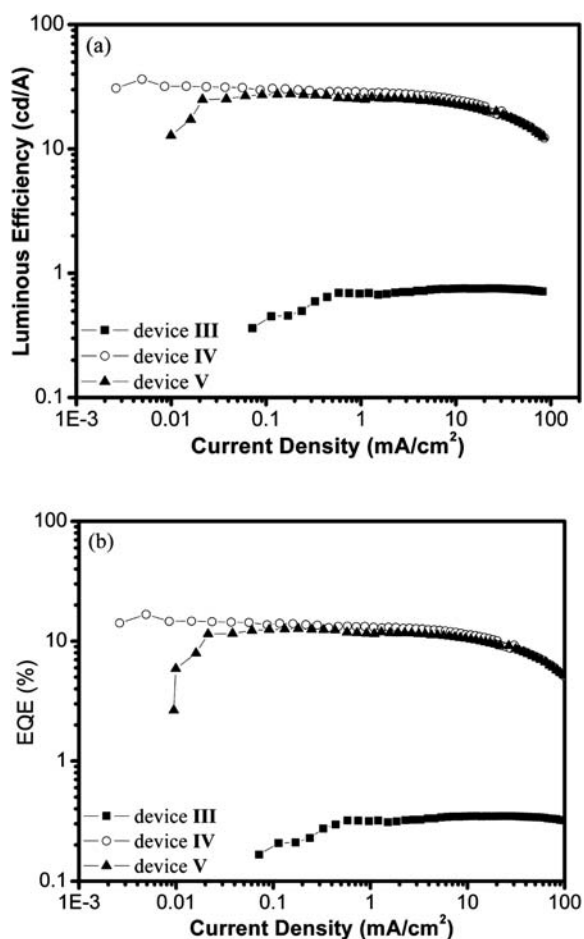


**Fig. 10** The current density dependence of the luminous efficiency (a) and EQE (b) of the TPCz-based device **III–V**.

$\delta$  8.13 (d,  $J = 7.5$  Hz, 2H), 7.72 (d,  $J = 8.4$  Hz, 2H), 7.45 (d,  $J = 8.4$  Hz, 2H), 7.35–7.41 (m, 4H), 7.29 (t,  $J = 7.8$  Hz, 2H).

**Synthesis of 4,4',4''-tri(*N*-carbazolyl)triphenylphosphine oxide (TCTP).** *n*-butyllithium (2.5 M  $\times$  7.5 mL, 18.8 mmol) was slowly added at  $-78$  °C to a solution of **1** (5.5 g, 17.1 mmol) in THF (80 mL). The reaction was kept at this temperature for 3 h, and then 0.48 mL (5.5 mmol) of trichlorophosphine was added. The resulting mixture was further stirred for 3 h more at  $-78$  °C before quenching with 4 mL of methanol. Water was added, and the mixture was extracted with  $\text{CH}_2\text{Cl}_2$ , washed with water, and dried over  $\text{Na}_2\text{SO}_4$ . After the solvent had been completely removed, 30% hydrogen peroxide (6 mL) and  $\text{CH}_2\text{Cl}_2$  (20 mL) were added to the obtained residue and they were stirred overnight at room temperature. The organic layer was separated and washed with water and then brine. The extract was evaporated to dryness, and the residue was purified by column chromatography on silica gel using dichloromethane–methanol (50 : 1 to 20 : 1) as eluent to give 4,4',4''-tri(*N*-carbazolyl)triphenylphosphine oxide (TCTP) with a yield of 41% (1.7 g).  $^1\text{H}$  NMR ( $\text{CDCl}_3$ ):  $\delta$  8.09 (d,  $J = 7.5$  Hz, 6H), 8.03 (dd,  $J = 10.0, 3.2$  Hz, 6H), 7.79 (dd,  $J = 2.2, 8.5$  Hz, 6H), 7.49 (d,  $J = 8.2$  Hz, 6H), 7.38 (t,  $J = 8.2$  Hz, 6H), 7.26 (t,  $J = 7.5$  Hz, 6H).  $^{13}\text{C}$  NMR ( $\text{CDCl}_3$ ):  $\delta$  141.8, 140.2, 133.9, 131.3, 129.9, 126.8, 126.3, 123.9, 120.6, 109.7.  $^{31}\text{P}$  NMR ( $\text{CDCl}_3$ ):  $\delta$  27.5. Anal. calcd for  $\text{C}_{54}\text{H}_{36}\text{N}_3\text{OP}$ : C, 83.81; H, 4.69; N, 5.43. Found: C, 84.03; H, 4.59; N, 5.08. MALDI-TOF ( $m/z$ ): 774.3 [ $\text{M}^+ + \text{H}$ ].

**Synthesis of 9-(4'-bromophenyl)-3,6-dibromocarbazole (2).** To a solution of **1** (1.6 g, 5.0 mmol) in DMF (20 mL) at 0 °C, NBS (2.0 g, 11.0 mmol) in DMF (10 mL) was added drop-wise. The mixture was stirred for 3 h at room temperature. Then, water was added to the mixture to give a white precipitate. After filtration and drying, the obtained white solid was recrystallized from petroleum to afford 9-(4'-bromophenyl)-3,6-dibromocarbazole (**2**) with a yield of 86% (2.1 g).  $^1\text{H}$  NMR ( $\text{CDCl}_3$ ):  $\delta$  8.19 (d,  $J = 1.8$  Hz, 2H), 7.74 (d,  $J = 8.7$  Hz, 2H), 7.51 (dd,  $J = 8.7, 1.8$  Hz, 2H), 7.38 (d,  $J = 8.4$  Hz, 2H), 7.22 (d,  $J = 8.7$  Hz, 2H).

**Synthesis of 3,6-bis(diphenylphosphoryl)-9-(4'-(diphenylphosphoryl)phenyl)carbazole (TPCz).** *n*-butyllithium (2.5 M, 5.3 mL, 13.2 mmol) was slowly added at  $-78$  °C to a solution of **2** (1.9 g, 4.0 mmol) in THF (100 mL). The reaction was kept at this temperature for 3 h, and then 2.4 mL (13.2 mmol) of chlorodiphenylphosphine was added. The resulting mixture was stirred for 3 h more at  $-78$  °C before quenching with 5 mL of methanol. Water was added, and the mixture was extracted with  $\text{CH}_2\text{Cl}_2$ , washed with water, dried over  $\text{Na}_2\text{SO}_4$ . After the solvent had been completely removed, 30% hydrogen peroxide (15 mL) and  $\text{CH}_2\text{Cl}_2$  (20 mL) were added to the obtained residue and they were stirred overnight at room temperature. The organic layer was separated and washed with water and then brine. The extract was evaporated to dryness, and the residue was purified by column chromatography on silica gel using ethyl acetate–methanol (20 : 1) as eluent to give 3,6-bis(diphenylphosphoryl)-9-(4'-(diphenylphosphoryl)phenyl)carbazole (TPCz) with a yield of 47% (1.6 g).  $^1\text{H}$  NMR ( $\text{CDCl}_3$ ):  $\delta$  8.45 (d,  $J = 12.3$  Hz, 2H), 7.95 (d,  $J = 8.4$  Hz, 1H), 7.91 (d,  $J = 8.1$  Hz, 1H), 7.65–7.79 (m, 16H), 7.44–7.62 (m, 20H).  $^{13}\text{C}$  NMR ( $\text{CDCl}_3$ ):  $\delta$  142.8, 139.7, 134.2, 133.7,

132.6, 132.3, 132.2, 132.0, 131.2, 130.3, 128.8, 128.5, 126.8, 125.7, 125.3, 123.9, 123.3, 110.2.  $^{31}\text{P}$  NMR ( $\text{CDCl}_3$ ):  $\delta$  28.4, 30.1. Anal. calcd for  $\text{C}_{54}\text{H}_{40}\text{NO}_3\text{P}_3$ : C, 76.86; H, 4.78; N, 1.66. Found: C, 75.90; H, 4.77; N, 1.58. MALDI-TOF ( $m/z$ ): 844.2 [ $\text{M}^+ + \text{H}$ ].

## Measurement and characterization

$^1\text{H}$  NMR,  $^{13}\text{C}$  NMR and  $^{31}\text{P}$  NMR spectra were recorded with Bruker Avance 300 NMR spectrometer. Elemental analysis was performed using a Bio-Rad elemental analysis system. MALDI/TOF (matrix assisted laser desorption ionization/time-of-flight) mass spectra were performed on AXIMA CFR MS apparatus (COMPACT). Thermal gravimetric analysis (TGA) and differential scanning calorimetry (DSC) were performed under a flow of nitrogen with a Perkin-Elmer-TGA 7 and Perkin-Elmer-DSC 7 system, respectively. UV-vis absorption and photoluminescence spectra were measured with a Perkin-Elmer Lambda 35 UV/vis spectrometer and a Perkin-Elmer LS 50B spectrofluorometer, respectively. Phosphorescence spectra at 77 K were measured in a toluene–ethanol–methanol (5 : 4 : 1) solvent mixture. The highest energy peaks in the phosphorescence spectra at 77 K were referred to as the  $S_0^v=0 \leftarrow T_1^v=0$  transitions. Cyclic voltammetry (CV) experiments were performed on an EG&G 283 (Princeton Applied Research) potentiostat/galvanostat system. With regard to the energy level of the ferrocene reference (4.8 eV relative to the vacuum level), the HOMO and LUMO energy levels were calculated according to the following three equations: HOMO =  $-e(4.8 \text{ V} + E^{\text{ox}})$ , LUMO =  $-e(4.8 \text{ V} + E^{\text{red}})$ , and LUMO =  $E_g + \text{HOMO}$ . Here,  $E^{\text{ox}}$  and  $E^{\text{red}}$  were taken from the onset of the oxidation and reduction potential, respectively, and  $E_g$  was the optical band gap estimated from the onset of the absorption spectrum.<sup>9</sup> Theoretical calculations were performed using the Gaussian 03 program, and the chemical structures of TCTP and TPCz were fully optimized by density functional theory (DFT) using Beck's three-parameterized Lee–Yang–Parr exchange functional (B3LYP) with 6-31G\* basis sets.

## Device fabrication and testing

*N,N'*-bis((1-naphthyl)-*N,N'*-diphenyl-1,1'-biphenyl-4,4'-diamine (NPB) was purchased from Acros, while TCTA, *N,N'*-dicarbazolyl-3,5-benzene (mCP), 3-(4-biphenyl)-4-phenyl-5-(4-*tert*-butylphenyl)-1,2,4-triazole (TAZ) and iridium(III)[bis(4,6-difluorophenyl)pyridinato-*N,C'*]-picolate (FIRpic) were prepared in our lab. OLEDs were fabricated by means of vacuum deposition with ITO glass as the substrate (10  $\Omega/\square$ ). The ITO surface was degreased in an ultrasonic solvent bath and then dried at 120 °C prior to use. For device **I**, 70 nm thick NPB film followed by 5 nm thick TCTA film was first deposited on the ITO glass substrates. 8 wt% FIRpic and TCTP were co-evaporated to form a 20 nm emitting layer (EML). Successively, TAZ (40 nm), LiF (1 nm) and Al (100 nm) were evaporated at a base pressure less than  $10^{-6}$  Torr (1 Torr = 133.32 Pa). For comparison, device **II** was also fabricated with TCTA as the host instead of TCTP. Device **III** was similarly assembled with the sequence: ITO on glass substrate, 65 nm of NPB, 20 nm of the EML made of TPCz doped with 8 wt% FIRpic, 40 nm of TAZ, 1 nm of LiF and 100 nm Al. To improve the device performance, device **IV** was

prepared through inserting an additional mCP electron-blocking layer (10 nm) between NPB and the EML. For device V, TPCz was used as the electron-transporting layer instead of TAZ compared with device IV. The active area of all the devices is 16 mm<sup>2</sup>. The electroluminescence (EL) spectra and Commission Internationale de L'Eclairage (CIE) coordinates were measured using a PR650 spectra colorimeter. The current–voltage and brightness–voltage curves of devices were measured using a Keithley 2400/2000 source meter and a calibrated silicon photodiode. All the experiments and measurements were carried out at room temperature under ambient conditions.

## Acknowledgements

The authors are grateful to the National Natural Science Foundation of China (No. 50803062), Science Fund for Creative Research Groups (No. 20621401), and 973 Project (2009CB623601) for financial support of this research. We also thank Prof. Jingping Zhang in Northeast Normal University for her help on the theoretical calculations.

## References

- 1 J. Kido, M. Kimura and K. Nagai, *Science*, 1995, **267**, 1332.
- 2 S. Reineke, F. Lindner, G. Schwartz, N. Seidler, K. Walzer, B. Lüssem and K. Leo, *Nature*, 2009, **459**, 234.
- 3 J. Ding, J. Gao, Q. Fu, Y. Cheng, D. Ma and L. Wang, *Synth. Met.*, 2005, **155**, 539.
- 4 J. Ding, J. Lü, Y. Cheng, Z. Xie, L. Wang, X. Jing and F. Wang, *Adv. Funct. Mater.*, 2008, **18**, 2754.
- 5 M. Ikai, S. Tokito, Y. Sakamoto, T. Suzuki and Y. Taga, *Appl. Phys. Lett.*, 2001, **79**, 156.
- 6 J. Ding, J. Gao, Y. Cheng, Z. Xie, L. Wang, D. Ma, X. Jing and F. Wang, *Adv. Funct. Mater.*, 2006, **16**, 575.
- 7 J. Ding, B. Wang, Z. Yue, B. Yao, Z. Xie, Y. Cheng, L. Wang, X. Jing and F. Wang, *Angew. Chem., Int. Ed.*, 2009, **48**, 6664.
- 8 H. Sasabe, T. Chiba, S. –J. Su, Y. –J. Pu, K. –i. Nakayama and J. Kido, *Chem. Commun.*, 2008, 5821.
- 9 J. Ding, B. Zhang, J. Lü, Z. Xie, L. Wang, X. Jing and F. Wang, *Adv. Mater.*, 2009, **21**, 4983.
- 10 Z. Ge, T. Hayakawa, S. Ando, M. Ueda, T. Akiike, H. Miyamoto, T. Kajita and M. –a. Kakimoto, *Adv. Funct. Mater.*, 2008, **18**, 584.
- 11 Y. Shirota, *J. Mater. Chem.*, 2000, **10**, 1.
- 12 R. J. Holmes, S. R. Forrest, Y. –J. Tung, R. C. Kwong, J. J. Brown, S. Garon and M. E. Thompson, *Appl. Phys. Lett.*, 2003, **82**, 2422.
- 13 M. Sudhakar, P. I. Djurovich, T. E. Hogen-Esch and M. E. Thompson, *J. Am. Chem. Soc.*, 2003, **125**, 7796.
- 14 S. H. Kim, J. Jang, K. S. Yook and J. Y. Lee, *Appl. Phys. Lett.*, 2008, **92**, 023513.
- 15 N. C. Giebink and S. R. Forrest, *Phys. Rev. B: Condens. Matter Mater. Phys.*, 2008, **77**, 235215.
- 16 T. H. Huang, J. T. Liu, L. Y. Chen, Y. T. Lin and C. C. Wu, *Adv. Mater.*, 2006, **18**, 602.
- 17 Z. H. Li, M. S. Wong, H. Fukutani and Y. Tao, *Org. Lett.*, 2006, **8**, 4271.
- 18 Y. Tao, Q. Wang, Y. Shang, C. Yang, L. Ao, J. Qin, D. Ma and Z. Shuai, *Chem. Commun.*, 2009, 77.
- 19 Q. Wang, J. Ding, D. Ma, Y. Cheng and L. Wang, *Appl. Phys. Lett.*, 2009, **94**, 103503.
- 20 G. He, M. Pfeiffer, K. Leo, M. Hofmann, J. Birnstick, R. Pudzich and J. Salbeck, *Appl. Phys. Lett.*, 2004, **85**, 3911.
- 21 P. E. Burrows, A. Padmaperuma, L. S. Sapochak, P. Djurovich and M. E. Thompson, *Appl. Phys. Lett.*, 2006, **88**, 183503.
- 22 A. B. Padmaperuma, L. S. Sapochak and P. E. Burrows, *Chem. Mater.*, 2006, **18**, 2389.
- 23 L. S. Sapochak, A. B. Padmaperuma, X. Cai, J. L. Male and P. E. Burrows, *J. Phys. Chem. C*, 2008, **112**, 7989.
- 24 S. O. Jeon, K. S. Yook, C. W. Joo and J. Y. Lee, *Adv. Funct. Mater.*, 2009, **19**, 3644.
- 25 S.-J. Su, H. Sasabe, T. Takeda and J. Kido, *Chem. Mater.*, 2008, **20**, 1691.
- 26 C. Adachi, M. A. Baldo and S. R. Forrest, *J. Appl. Phys.*, 2000, **87**, 8049.
- 27 M. A. Baldo, C. Adachi and S. R. Forrest, *Phys. Rev. B: Condens. Matter Mater. Phys.*, 2000, **62**, 10967.
- 28 C. Wu, P. I. Djurovich and M. E. Thompson, *Adv. Funct. Mater.*, 2009, **19**, 3157.
- 29 M. Watanabe, M. Nishiyama, T. Yamamoto and Y. Koie, *Tetrahedron Lett.*, 2000, **41**, 481.